PHILOSOPHICAL TRANSACTIONS OF THE ROYAL SOCIETY B BIOLOGICAL SCIENCES

Magnetization Densities and Electronic States in Crystals

P. Jane Brown, J. B. Forsyth and R. Mason

Phil. Trans. R. Soc. Lond. B 1980 **290**, 481-495
doi: 10.1098/rstb.1980.0109

Phil. Trans. R. Soc. Lond. B **290**, 481–495 (1980)
Printed in Great Britain

Magnetization densities and electronic states in crystals

By P. Jane Brown†, J. B. Forsyth‡ and R. Mason§, F.R.S.

† *Institut Max von Laue – Paul Langevin, Avenue des Martyrs, 38042 Grenoble cedex, France.*

‡ *Science Research Council, Rutherford Laboratory, Chilton, Didcot, Oxon. OX11 0QX, U.K.*

§ *Now Sir Ronald Mason, School of Molecular Sciences, Sussex University, Falmer, Brighton, Sussex, U.K.*

The classical polarized neutron technique provides an extremely sensitive method for studying magnetization distributions in crystalline materials. In the transition metals and their compounds it is recognized that the d electrons act both as valence electrons and as carriers of the magnetism. This dual role implies that the magnetization distribution can give information about the behaviour of valence electrons. The pioneering work in this field yielded new insight into the behaviour of the magnetic elements themselves.

The paper begins with an introduction to the elastic magnetic scattering of neutrons, the electronic origin of magnetization density and the polarized neutron technique itself. A brief survey of earlier work in the important areas of application is followed by more detailed discussion of three recent experiments: the determination of the paramagnetic form factor of technetium, a study of orbital effects in a ferrimagnetic vanadium salt ($K_5V_3F_{14}$) and the spin density and bonding in the $[CoCl_4]^{2-}$ ion.

1. Introduction

At the start of this meeting it is perhaps not out of place to recall some of the properties of the neutron. It is a neutral particle with mass not very different from that of the hydrogen atom; it has a magnetic dipole moment of 1.9 nuclear magnetons but to a close approximation no electric dipole moment. The neutron interacts with atomic nuclei through the strong nuclear interaction, and with electrons by virtue of its magnetic moment. It is this second interaction that is of prime interest for this paper. Since the neutron is scattered by its magnetic interaction with electrons, the measurement of magnetic scattering enables information about the magnetic properties of solids and in particular the distribution of electronic magnetization to be determined.

Within the first Born approximation, elastic scattering cross sections may be written in terms of the Fourier transform of the interaction potential. Thus

$$\mathrm{d}\sigma/\mathrm{d}\omega \propto \int \psi^* V(\boldsymbol{r})\, \mathrm{e}^{\mathrm{i}\boldsymbol{k}\cdot\boldsymbol{r}} \psi \,\mathrm{d}r^3. \tag{1.1}$$

For neutron magnetic scattering the interaction potential is related directly to the magnetic flux density, $\boldsymbol{B}$, in the scatterer and through that by Gauss's theorem to the magnetization density $\boldsymbol{M}(\boldsymbol{r})$ defined as the magnetic moment per unit volume. A magnetic structure factor $\boldsymbol{M}(\boldsymbol{K})$ can be defined such that

$$\boldsymbol{M}(\boldsymbol{K}) = \int \boldsymbol{M}(\boldsymbol{r})\, \mathrm{e}^{\mathrm{i}\boldsymbol{k}\cdot\boldsymbol{r}} \,\mathrm{d}r^3. \tag{1.2}$$

Then the magnetic elastic scattering cross section for unpolarized neutrons is given by

$$\partial\sigma/\partial\omega \propto |\hat{\boldsymbol{k}} \times \boldsymbol{M}(\boldsymbol{k}) \times \hat{\boldsymbol{k}}|^2 = |\boldsymbol{M}_\perp(\boldsymbol{k})|^2. \tag{1.3}$$

$\boldsymbol{M}_\perp(\boldsymbol{k})$ is the generalized magnetic interaction vector and it is this quantity, its square or its components that can be measured in a magnetic scattering experiment.

2. The electronic origin of the magnetization density

The magnetization density in a crystal is due both to the intrinsic magnetic moment of electrons (the electron spin) and to the magnetic moment generated by moving electrons (orbital magnetization). In most materials, paired electrons generate equal and opposite magnetic moments so that the net magnetization density is everywhere zero, but in magnetic or magnetized matter some electrons are unpaired. In such cases the magnetization density due to spin reflects the spatial distribution of the unpaired electrons, but that due to their orbital motion is less simply interpreted.

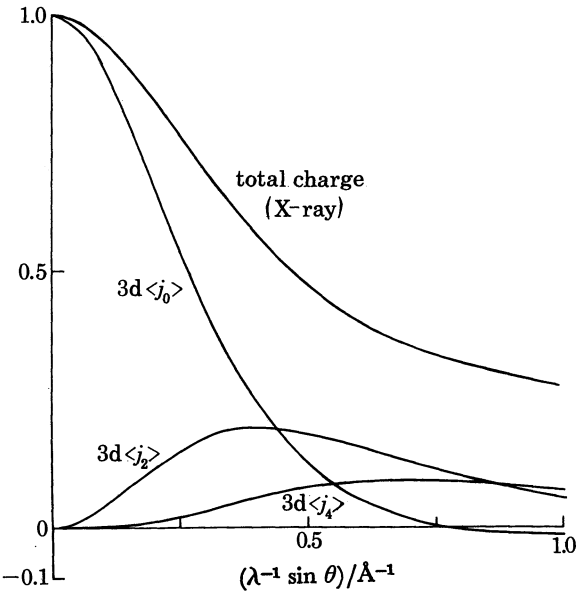

Figure 1. The total charge and 3d form factors for the Mn^{2+} ion.

In some cases it may be appropriate to consider the total magnetization as the sum of distributions from individual atoms, and it is then useful to define magnetic form factors for each atom. A magnetic form factor is defined as

$$f(\boldsymbol{k}) = (\int m(\boldsymbol{r})\, e^{i\boldsymbol{k}\cdot\boldsymbol{r}}\, d\boldsymbol{r}^3)/(\int m(\boldsymbol{r})\, d\boldsymbol{r}^3), \tag{2.1}$$

where $m(\boldsymbol{r})$ is the magnetization density associated with the atom. The magnetic structure factor can readily be expressed in terms of the form factors as

$$\boldsymbol{M}(\boldsymbol{k}) = \sum_n f_n(\boldsymbol{k})\, \boldsymbol{M}_n\, e^{i\boldsymbol{k}\cdot\boldsymbol{r}_n}. \tag{2.2}$$

Here $f_n(\boldsymbol{k})$ is the form factor for the nth atom at distance r_n from the origin, and $\boldsymbol{M}_n$ is its magnetic moment; the sum is over all atoms in the crystal. When the magnetization is due to

electrons in a single unfilled shell, the form factor may be written as

$$f(\boldsymbol{k}) = \sum_l A_l(\hat{\boldsymbol{k}})\,\langle j_l(|\boldsymbol{k}|)\rangle, \tag{2.3}$$

where

$$\langle j_l(\boldsymbol{k})\rangle = \int_0^\infty U^2(r)\, j_l(kr)\,\mathrm{d}r. \tag{2.4}$$

Here $j_l(kr)$ is the spherical Bessel function of order l and $U^2(r)$ the radial distribution function of electrons in the open shell. The $A_l(\hat{\boldsymbol{k}})$ are coefficients that depend both on the direction of the scattering vector, $\boldsymbol{k}$, and on the magnetic configuration. For a spherically symmetric spin-only ion such as the Mn^{2+} ^{5}d configuration, only A_0 is finite. For the general spin-only case with d electrons, A_0, A_2 and A_4 are non-zero. An approximation to the spherical form factor valid for small $\boldsymbol{k}$ when orbital moment is present is given by the dipole approximation (Marshall & Lovesey 1971)

$$f(\boldsymbol{k}) = 2S\langle j_0(k)\rangle + L(\langle j_0(k)\rangle + \langle j_2(k)\rangle). \tag{2.5}$$

Figure 1 shows the k dependence of the three integrals $\langle j_0\rangle$ $\langle j_2\rangle$ $\langle j_4\rangle$ for 3d electrons in the Mn^{2+} ion. Only $\langle j_0\rangle$ is non-zero at $k = 0$, so the coefficient A_0 measures the net magnetic moment of the ion. Figure 1 also shows the X-ray form factor for Mn^{2+} to which all the electrons contribute; the contribution from the core electrons makes this form factor larger at high k than the magnetic form factor. One may compare the absolute magnitudes of the scattering factors at $\lambda^{-1}\sin\theta = \sin\theta/\lambda = 0.25$ Å^{-1}† for X-rays and for magnetic and nuclear scattering of neutrons; these are 5.5, 0.74 and -0.37×10^{-12} cm respectively.

3. Scattering of polarized neutrons

The scattering cross section of (1.3) is the sum of two partial cross sections that correspond to scattering with and without a change of neutron spin direction. There can be interference between nuclear and magnetic scattering if there is no change of spin direction and for an incident beam polarized parallel to $\hat{\boldsymbol{\lambda}}$, the spin-non-flip cross section is,

$$\partial\sigma/\partial\omega(\uparrow\uparrow) = |N(\boldsymbol{k}) + \hat{\boldsymbol{\lambda}}\cdot\boldsymbol{M}_\perp(\boldsymbol{k})|^2. \tag{3.1}$$

Only magnetic scattering can reverse the neutron spin direction in Bragg scattering if there is no nuclear polarization and the spin flip cross section is simply

$$\partial\sigma/\partial\omega(\uparrow\downarrow) = |\hat{\boldsymbol{\lambda}}\times\boldsymbol{M}_\perp(\boldsymbol{k})|^2. \tag{3.2}$$

An instrument for doing polarized neutron diffraction experiments is indicated schematically in figure 2. A monochromatic polarized neutron beam is produced by Bragg reflexion of polychromatic unpolarized neutrons from the reactor by a polarizing crystal. The ideal polarizing crystal has $N(\boldsymbol{k}) = \boldsymbol{M}(\boldsymbol{k})$ so that by (3.1) it has zero cross section for neutrons polarized antiparallel to $\boldsymbol{M}(\boldsymbol{k})$ and a large cross section for the reverse polarization. The polarization is maintained in the flight path to the specimen by magnetic guides, producing fields in the polarization direction. At some point in this path a 'spin flipper' is introduced; this may be an r.f. coil tuned to the Larmor frequency, as in the original diffractometer, or one of a number of other devices. The function of the spin flipper is to reverse the polarization when it is 'on' and allow the neutrons to pass unchanged when it is 'off'. In a polarized neutron experiment, the diffractometer and sample are set so that the peak of a Bragg reflexion

† 1 Å = 10^{-10} m = 10^{-1} nm.

enters the detector and the ratio between the counting rates for the two polarization states is measured. This ratio, commonly known as the 'flipping ratio' is recorded for each reflexion and these ratios are the 'raw data' of the experiment. From (3.1) and (3.2) it can be shown that the flipping ratio, R, is

$$\frac{|N(\boldsymbol{k})|^2+|\boldsymbol{M}(\boldsymbol{k})|^2+N(\boldsymbol{k})\,\hat{\boldsymbol{\lambda}}\cdot\boldsymbol{M}^*(\boldsymbol{k})+N^*(\boldsymbol{k})\,\hat{\boldsymbol{\lambda}}\cdot\boldsymbol{M}(\boldsymbol{k})}{|N(\boldsymbol{k})|^2+|\boldsymbol{M}(\boldsymbol{k})|^2-N(\boldsymbol{k})\,\hat{\boldsymbol{\lambda}}\cdot\boldsymbol{M}^*(\boldsymbol{k})-N^*(\boldsymbol{k})\,\hat{\boldsymbol{\lambda}}\cdot\boldsymbol{M}(\boldsymbol{k})}. \tag{3.3}$$

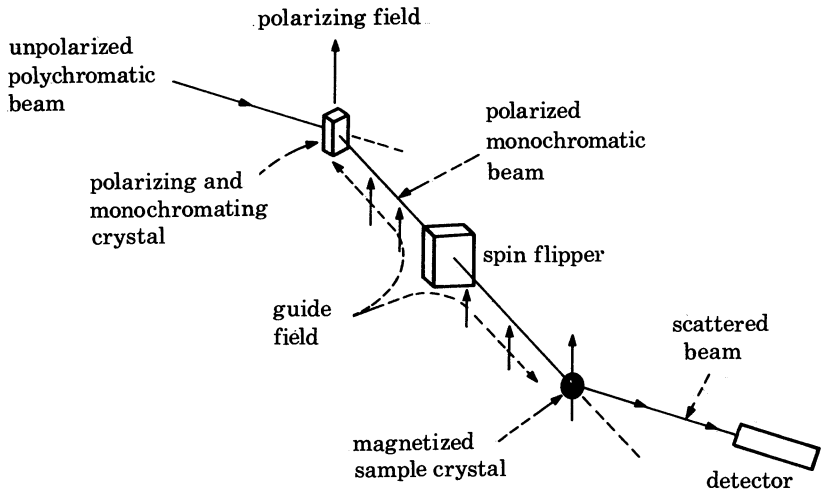

FIGURE 2. Schematic representation of an instrument for polarized neutron diffraction.

In the simple case that both $N(\boldsymbol{k})$ and $\boldsymbol{M}_\perp(\boldsymbol{k})$ are real (centrosymmetric structures) and the polarization is parallel to the magnetization and perpendicular to the scattering vector, the ratio becomes

$$R=\frac{N(k)^2+M(k)^2+2N(k)\,M(k)}{N(k)^2+M(k)^2-2N(k)\,M(k)}=\left(\frac{1+\gamma}{1-\gamma}\right)^2, \tag{3.4}$$

where

$$\gamma=\frac{M(k)}{N(k)}.$$

In general, R can only be different from unity if there are magnetic and nuclear scattering in the same reflexion so that the cross term in (3.4) is non-zero. This condition is satisfied if any part of the magnetization has the periodicity of the nuclear structure, as in a ferromagnet or a paramagnet in an applied field. It is not satisfied by antiferromagnetic structures in which the magnetic unit cell is some multiple of the chemical one.

The ratio γ can be derived from the flipping ratio, R, by solving the quadratic equation (3.4). The result, which assumes complete polarization and perfect spin reversal, is

$$\gamma=\{R+1\pm\sqrt{(4R)}\}/(R-1). \tag{3.5}$$

The choice of root depends on whether the absolute magnitude of the magnetic scattering is greater or less than that of the nuclear scattering. There is no uncertainty in the sign of γ, which depends on whether the ratio R is greater than or less than unity. This means that the polarized neutron technique fixes the relative phases of magnetic and nuclear scattering experimentally in centro-symmetric structures. The form of (3.5) shows that γ is not well determined by R when γ is close to 1. In this region, integrated intensity measurements give

better accuracy. However, it is one of the major advantages of the polarized technique that integrated intensities are not needed and it is the ratio between the peak counting rates for the reflexion that is measured. In most cases magnetic neutron scattering is much weaker than nuclear scattering and $|\gamma|$ is significantly less than one. For small γ, (3.5) can be simplified as

$$R = 1+4\gamma. \tag{3.6}$$

To show the enhanced sensitivity of the polarized technique for measurement of small magnetic scattering, (3.6) can be compared with the fraction of the integrated intensity due to magnetic scattering:

$$\Delta I/I = 1+\gamma^2. \tag{3.7}$$

The polarized neutron technique can be used to measure extremely small γ since down to 0.1% accuracy or better there is little except the counting statistics to limit the accuracy with which R can be measured. Measurements of very small γ values do, however, require long counting times and high incident intensity as is shown in table 1. To give some idea of the orders of magnitude involved, the counting rate from a strong reflexion of a simple crystal some tens of cubic millimetres in volume will probably not exceed 10^4/s which implies measurement times per reflexion of 2 min, 3 h and 12 days for the three cases of table 1.

TABLE 1. COUNTING REQUIREMENTS FOR MEASUREMENT OF SMALL γ IN POLARIZED NEUTRON EXPERIMENTS

(For small γ, $\Delta I/I = 1+\gamma^2$, whereas $R = 1+4\gamma$.)

γ	$\Delta I/I$	$R-1$	count for 5% error in γ
0.01	1×10^{-4}	4×10^{-2}	2×10^{6}
0.001	1×10^{-6}	4×10^{-3}	2×10^{8}
0.0001	1×10^{-8}	4×10^{-4}	2×10^{10}

4. A SURVEY OF MEASUREMENTS WITH THE 'CLASSICAL' POLARIZED NEUTRON TECHNIQUE

The 'classical' polarized neutron technique was first described by Nathans *et al.* (1959). Early investigations were confined to simple systems that are ferromagnetic at ambient temperatures, and included detailed studies of the form factors of the metals iron, cobalt and nickel. The development of superconducting magnets and the availability of higher polarized neutron fluxes enabled the technique to be extended to paramagnetic materials and to more complex systems. Many studies have been carried out on the rare earth and actinide elements, their compounds and their alloys, which have yielded new insight into the magnetic states of these materials. In this paper we shall, however, confine our attention to the transition metals and their compounds in which the d electrons not only give rise to magnetism but also play an important rôle in chemical bonding.

Paramagnetic metals of the 3d, 4d and 5d series have been studied at the Oak Ridge National Laboratory in the U.S.A. (Moon *et al.* 1976). Single crystals of the metals were subjected to fields of up to 10 T and the magnetic scattering of the aligned paramagnetic moment was measured. The results provide a very sensitive test of band structure calculations because the magnetic structure factors depend strongly on the eigenfunctions rather than just on the eigenvalues of the electron wave functions.

PHILOSOPHICAL TRANSACTIONS OF THE ROYAL SOCIETY B BIOLOGICAL SCIENCES

Relatively few studies of ordered magnetic salts have been made because these usually order antiferromagnetically, and even when mixed magnetic and nuclear reflexions occur, the existence of magnetic domains insensitive to applied fields complicates the experiments. Exceptions include the weak canted ferromagnets typified by $MnCO_3$, in which the spatial distribution of the small ferromagnetic moment has been measured (Brown & Forsyth 1967). Metamagnetic layered halides such as $FeCl_2$ have also been studied, as have some ferromagnetic mixed oxides (Bonnet *et al.* 1978; Rakhecha & Satya Murthy 1978). The interpretation of the results of these studies has been in terms of ligand field theory of the magnetic ions with the use of parameters obtained from resonance, spectroscopic and bulk magnetic measurements. Differences between the predictions of the models and the measurements demonstrate transfer of magnetic moment to ligand ions and enable simple covalency parameters to be deduced (Hubbard & Marshall 1965).

The availability of higher neutron fluxes, higher magnetic fields and a developing formalism for calculating magnetic structure factors has stimulated the study of more complex magnetic systems in which significant orbital scattering may be present and of more complex chemical systems such as organometallic compounds.

To illustrate the current status of the technique, we shall describe in rather more detail three recent experiments carried out at the Institut Laue–Langevin that exemplify three different areas of application. These are the determination of the paramagnetic form factor of technetium (Radhakrishna & Brown 1979), a study of orbital effects in a ferrimagnetic vanadium salt (Forsyth & Brown 1979) and spin density and bonding in the $[CoCl_4]^{2-}$ ion (Figgis *et al.* 1979*a*).

5. The paramagnetic form factor of technetium

Technetium, which is the 4d analogue of manganese in the 3d and rhenium in the 5d transition metal series, does not occur naturally. It can be obtained from spent nuclear fuel as the radioactive isotope Tc^{99}, a soft β-emitter with a half life of 2×10^5 years. Technetium is a hexagonal close-packed metal; it has a paramagnetic susceptibility which remains essentially constant at 10^{-6} e.m.u./g† over the temperature range 80–1400 K. The form factor of the paramagnetic electrons in technetium is of interest because of the rather strange form factors found for other hexagonal close-packed transition metals such as scandium, titanium and yttrium in which the low angle reflexions do not fall on a smooth curve (Moon *et al.* 1976).

An applied field of 4.8 T at 100 K gives an aligned paramagnetic moment of $0.94 \times 10^{-3}\ \mu_B$ per atom of technetium, and the expected γ value at the lowest angle reflexion is about 2×10^{-4}. This shows that measurement of the paramagnetic scattering is at the lower limit of possibility. However, large single crystals have been grown by Kostorz & Mikhailovich (1970) and two were lent to us by the Oak Ridge National Laboratory. These crystals enabled us to achieve counting rates of up to 10^5/s and the rate used was limited only by the detector dead time. Thus with about 28 days measuring time we were able to obtain the flipping ratios of the eight lowest angle reflexions with an accuracy of around one part in 10^{-4}. At this level of precision in flipping ratio measurements, account must be taken of small systematic errors which may invalidate the results. An account of some of these errors is given by Moon *et al.* (1975). Because of the energy difference between the two neutron polarization states in high fields, and to the

† 1 e.m.u. of magnetic volume susceptibility $\approx 1/4\pi$ of 1 SI unit.

PHILOSOPHICAL TRANSACTIONS OF THE ROYAL SOCIETY B BIOLOGICAL SCIENCES

Stern–Gerlach bending of the beam as it traverses the inhomogeneous field regions, the reflexion curves of the two polarization states are not exactly superposed. This may give rise to spurious flipping ratios if the reflexion curve is sharp and the measurement is not made at the exact mean position of the two curves. In the present experiments, the reflexion curves were quite broad (0.25° f.w.h.m.) and an on-line maximization option in the diffractometer control package was used to ensure that the crystal was set to the centre of the reflexion before each measurement. The precision of the flipping ratios was estimated from the degree of reproducibility between repeated measurements of all available equivalent reflexions; in no case was the reproducibility found to be significantly different from that expected from counting statistics.

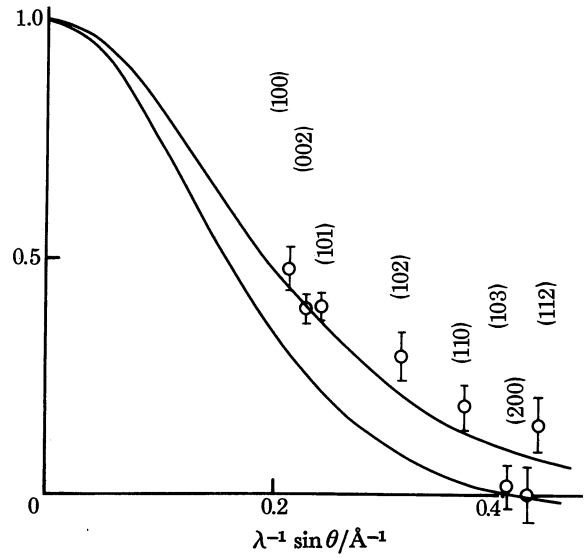

FIGURE 3. The paramagnetic form factor of technetium. The experimental points with their estimated errors are shown. The lower full curve corresponds to the spin-only form factor for Tc 4d electrons. The upper full curve corresponds to the dipole approximation for 70% orbital moment.

Other physical effects that must be taken into account before the paramagnetic structure factors can be obtained from the flipping ratios are extinction, Schwinger scattering and diamagnetism. To determine the degree of extinction a separate experiment with unpolarized neutrons was carried out. The integrated intensities of the reflexions were measured at 100 K in zero field and the results showed extinction to be negligible in the flipping ratios. The magnitude of the Schwinger scattering, which arises from the interaction between the neutrons' spin and the atomic electric field, is in this case of the same order of magnitude as the experimental uncertainty and so has been included. The same is true of the diamagnetic scattering, which is calculated from the second moment of the charge density (Stassis 1970). Once these effects have been removed, the resultant magnetic structure amplitudes are Fourier components of the paramagnetic magnetization density. They are converted to points on the paramagnetic form factor by dividing by the geometric structure factors and the value of the bulk magnetization per cell. The bulk magnetization is also corrected for the diamagnetic moment. The results are shown in figure 3: they fall on a reasonably smooth curve unlike those for scandium, yttrium and titanium. This confirms that the behaviour of these latter elements is due to their early positions in the transition series rather than to their hexagonal structures.

PHILOSOPHICAL TRANSACTIONS OF THE ROYAL SOCIETY B BIOLOGICAL SCIENCES

The experimental points lie well above the lower full curve of figure 3 which gives the spin-only form factor for Tc 4d electrons. This is not unexpected since a temperature-independent susceptibility may have an important Van-Vleck orbital component. The experimental data have been fitted to a Tc 4d form factor in the dipole approximation (equation (2.5)) allowing the ratio of spin to orbital moment to vary. The result suggests that 70% of the moment is orbital, and the resultant form factor is shown in the upper solid curve of figure 3. This model gives a reasonable account of the experimental data; further elaboration must await a good calculation of the technetium band structure.

This study of technetium is an example of the measurement of a very small magnetization in a very simple structure. The results will provide a stringent test of any band structure calculation.

6. Orbital effects in the magnetic scattering of $K_5V_3F_{14}$

Our next example comes from the study of strongly magnetic salts: it shows the dramatic way in which the magnetic scattering can depend on details of the ground state of the magnetic ion. We have already commented that the Mn^{2+} ion exhibits, to a good approximation, the spin-only moment of 5 μ_B and this is also true for the isoelectronic Fe^{3+} ion. Normally $Fe^{2+}(3d^6)$ and $Ni^{2+}(3d^8)$ ions have moments in which there is some 5–10% orbital contribution, and this proportion increases further for $Co^{2+}(3d^7)$. V^{3+} is an ion in which the 3d shell is less than half full ($3d^2$) and in which we may expect the orbital and spin components, L and S, to be opposed. The Hund's rule ground state is ^3F. The moment associated with the V^{3+} ions in V_2O_3 is 1.2 μ_B (Moon 1970) and this is evidence for a significant orbital contribution which reduces the spin-only moment of 2 μ_B. Balcar *et al.* (1973) have pointed out that the scattering of V^{3+} in V_2O_3 should be very anisotropic owing to the large orbital contribution. However, a crystallographic phase transition precludes a single crystal study of the magnetization density.

A detailed study is being made of the magnetization of V^{3+} in $K_5V_3F_{14}$, which is one of a series of fluorides having the general formula $A_5^+M_3^{3+}F_{14}^-$, in which A is an alkali metal (Na^+ or K^+) and M is a trivalent transition metal ion (Fe^{3+}, Co^{3+}, V^{3+}). The substances are ferrimagnetic and have chemical structures related to that of chiolite, $Na_5Al_3F_{14}$, which was first determined by Brosset (1938). Chiolite is tetragonal with space group P4/mnc. There are two formula units per unit cell, which has $a = 7.01$ Å and $c = 10.41 \pm 0.01$ Å. The preparation of $K_5V_3F_{14}$ single crystals has been described by Wanklyn *et al.* (1976) and bulk magnetization measurements show that it becomes ferrimagnetic below 18 K with a saturation magnetization at 0 K corresponding to 2.15 μ_B per formula unit (Cros *et al.* 1977). The crystals are not damaged by cooling to 4.2 K and two neutron studies have been made at that temperature.

Unpolarized beam diffraction data confirm that $K_5V_3F_{14}$ is isomorphous with chiolite and have enabled its atomic positional and thermal parameters to be determined. A second series of measurements were carried out with the classical polarized beam technique. Flipping ratios of some 1800 reflexions were measured at a wavelength of 0.933 Å. The specimen was in an external field of 1.5 T aligned parallel to the crystal rotation axis, which was [001]. Figure 4 shows that this is the easy direction of magnetization and 0.2 T is sufficient for saturation (Cros *et al.* 1977). The data were corrected for incomplete beam polarization and averaged over crystallographically equivalent reflexions to yield some 300 independent observations.

The atomic arrangement in $K_5V_3F_{14}$ is illustrated in figure 5. Two crystallographically

PHILOSOPHICAL TRANSACTIONS OF THE ROYAL SOCIETY B BIOLOGICAL SCIENCES

independent V^{3+} ions are octahedrally coordinated by fluorine atoms and form layers perpendicular to $\boldsymbol{c}$ centred about $z = 0$ and $z = \frac{1}{2}$. The two V(1) atoms at (000) and $(\frac{1}{2}\frac{1}{2}\frac{1}{2})$ have local symmetry 4/mmm and have moments that are opposed to those of the four V(2) atoms at $(\frac{1}{2}00)$, $(0\frac{1}{2}0)$, $(\frac{1}{2}0\frac{1}{2})$ and $(0\frac{1}{2}\frac{1}{2})$. The V(2) atoms have orthorhombic local symmetry, with the moment perpendicular to an octahedron edge. The potassium atoms lie between the layers at height $z = \frac{1}{4}$.

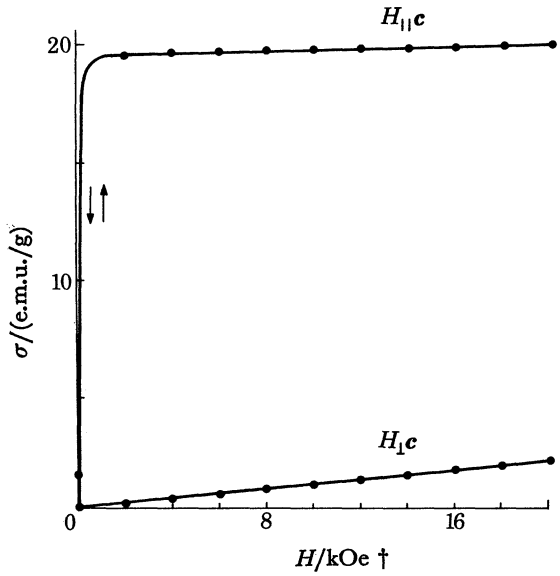

FIGURE 4. The variation of magnetization in $K_5V_3F_{14}$ at 4.2 K as a function of magnetic field H for H parallel and perpendicular to the $\boldsymbol{c}$ axis (Cros *et al.* 1977). † 1 kOe ≈ 79.58 kA m^{-1}.

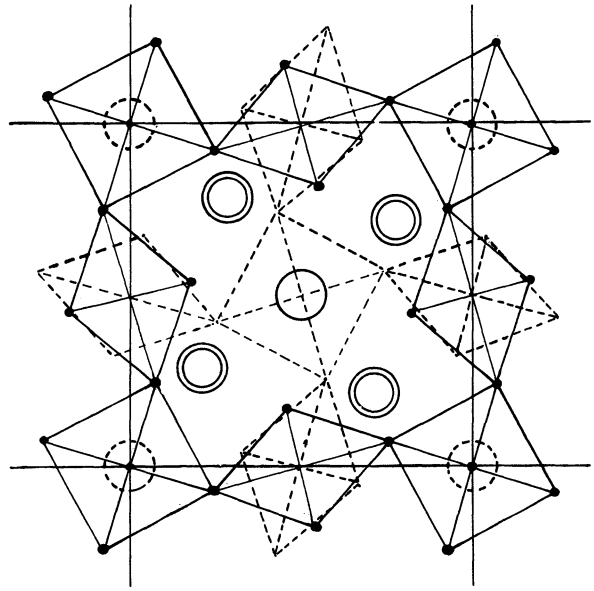

FIGURE 5. The structure of $K_5V_3F_{14}$ projected down [001]. The octahedra of fluorine atoms about the V(1) and V(2) sites are shown, the layer about $z = 0$ in full lines and the layer about $z = \frac{1}{2}$ in broken lines. Potassium atoms, shown as two concentric circles, are at heights $z = \frac{1}{4}$ and $\frac{3}{4}$.

PHILOSOPHICAL TRANSACTIONS OF THE ROYAL SOCIETY B BIOLOGICAL SCIENCES

The saturation magnetization of 2.15 μ_B, which arises from the difference in moments $2\,\mu_{V(2)}-\mu_{V(1)}$, might naïvely be associated with each ion having a moment close to its spin-only value of 2 μ_B. However, a preliminary analysis of the magnetic scattering amplitudes derived from the two neutron studies showed that both the magnitude and the form factor of the magnetic scattering from each of the independent V sites differ greatly from that to be expected from a spin-only ground state. In particular, the moment on the V(1) site is reduced to some 0.8 μ_B, whereas that on the V(2) site is about 1.5 μ_B. Furthermore, the form factor for the V(1) site reaches very large negative values around $\lambda^{-1}\sin\theta$ 0.4 Å^{-1}. However, the form

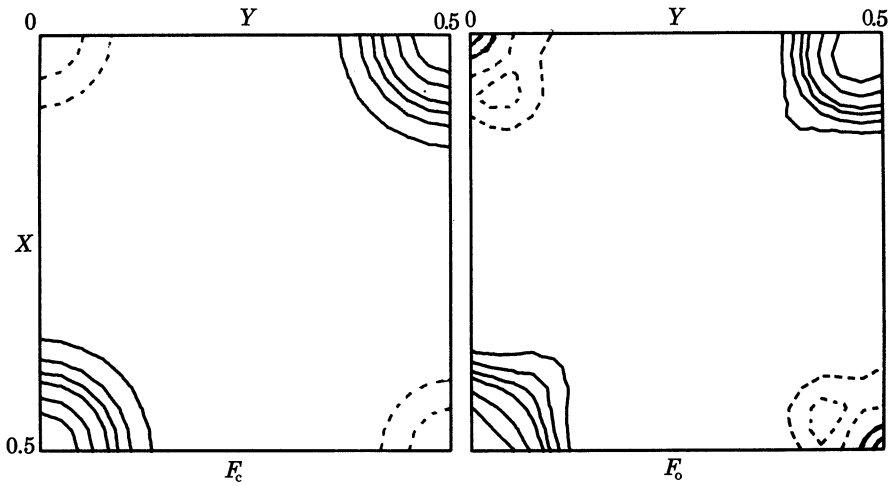

FIGURE 6. The calculated (F_c) and observed (F_o) [001] projections of the magnetization density in $K_5V_3F_{14}$. The calculated density corresponds to a model in which the vanadium ions have free-atom spin-only moments of V(1) = $-0.85\,\mu_B$ and V(2) = $1.5\,\mu_B$. The observed magnetization is very aspherical and the moment direction at the centre of the origin V(1) site is in fact oppositely directed to the majority of the magnetization at that site.

vector for the (h, k) even $l = 0$ reflexions, which have structure factors $\mu_{V(1)}+2\,\mu_{V(2)}$, approximates more closely to $\langle j_0\rangle$ for V^{3+}. These results may be partly understood in terms of the dipole approximation, since they would require a reduction in moment from 2 μ_B on the V(2) site that is about one-half the reduction for the V(1) site as is observed. The effect of the large orbital contribution on the magnetization density associated with the V(1) site is remarkable, as can be seen in figure 6, which shows its Fourier projection on (001). The projected density close to the atomic position is in fact oppositely directed to that in the outer regions of the ion.

The octahedral crystal field at the V^{3+} ions partially removes the orbital degeneracy of the ^3F state to leave a Γ_4 ground state which is further split by any tetragonal or orthorhombic distortions present at the V(1) and V(2) sites respectively and by the spin–orbit interaction. A calculation of the scattering which would be given by the V(1) atoms if they were in the pure ground state induced by the tetragonal distortion, namely

$$\{\epsilon|-3\rangle+(1-\epsilon^2)^{\frac{1}{2}}|+1\rangle\}\,|M_s=1\rangle \quad \text{with} \quad \epsilon=\sqrt{\tfrac{5}{8}}, \tag{6.1}$$

goes some way towards reproducing the sign change in the form factor at $\lambda^{-1}\sin\theta \approx 0.4$ Å^{-1}, but corresponds to 0.5 μ_B and not 0.8 μ_B/vanadium. A comparison between the observed and calculated structure factors for a limited number of reflexions to which only V(1) ions contribute is shown in figure 7. The calculated values correspond to a value for ϵ (equation

(6.1)) modified to give a moment of 0.8 μ_B. The large difference between values corresponding to different l cannot be reproduced by a simple wavefunction of this form. We are now extending the calculation to include the V(2) ions and a Hamiltonian containing the effects of crystal field, magnetic field and spin–orbit coupling. A least squares technique will be used to adjust the amplitudes of a suitable set of basis wavefunctions to minimize the differences between the observed and predicted values of the magnetic scattering amplitudes, and in this respect it resembles the pioneering work of Boucherle (1977) on rare earth intermetallic compounds. It is clear, even at this stage in the interpretation, that the large differences in behaviour of the magnetic scattering from the two very similar crystallographic atomic environments must provide a sensitive probe of their wavefunctions.

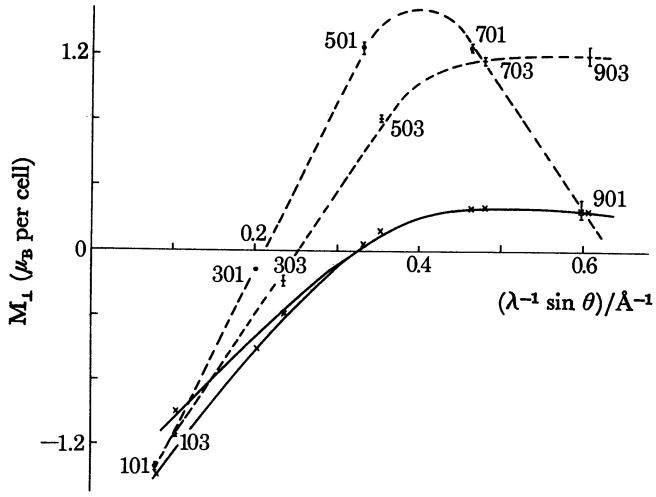

FIGURE 7. Observed and calculated magnetic scattering amplitudes from the V(1) ion in $K_5V_3F_{14}$. In the approximation of spherical distributions, V1 atoms only contribute to the $h0l$ reflexions with l odd. The calculated points (x) correspond to

$$\Psi_{V1} = 0.74|L_z = 3,\ \ S_z = 1\rangle + 0.67|L_z = -1,\ \ S_z = 1\rangle$$

which gives a magnetization of 0.8 μ_B/formula unit. The solid lines through the calculated values and the broken lines through the observations serve only to guide the eye.

7. SPIN DENSITIES IN PARAMAGNETIC MOLECULAR CRYSTALS

A direct study of covalence in paramagnetic molecules or ions is offered by the determination of spin density distribution in the crystal via Fourier transformation of magnetic structure factors determined by polarized neutron scattering techniques. A programme of studies of chemically significant compounds is under way (Figgis *et al.* 1979). However, the limitations attached to quantitative interpretations of Fourier series are well known and Varghese & Mason (1980) have developed the use of least squares multipole electron population analysis of the magnetic data and the relation of such an analysis to conventional orbital descriptions of molecular spin densities.

This approach is illustrated by a discussion of the polarized neutron data obtained from single crystals of Cs_3CoCl_5. Two independent sets of magnetic structure factors have been determined with the magnetization directed respectively along the 'a', ('b') and 'c' crystallographic axes (Figgis *et al.* 1980*a*). The crystallography of Cs_3CoCl_5 is well established, both by

PHILOSOPHICAL TRANSACTIONS OF THE ROYAL SOCIETY B BIOLOGICAL SCIENCES

X-ray and neutron diffraction methods at 300 and 4.2 K (Figgis *et al.* 1964, 1980*b*): the $(CoCl_4)^{2-}$ ions are embedded in a Cs^+, Cl^- matrix, the coordination geometry of the Co(II) ion being an axially distorted tetrahedron. The Co(II), d^7 ion has essentially a $^4A_2$ ground term; the bulk magnetization estimated from magnetic susceptibility measurements (van Stapele *et al.* 1966) gives a magnetic moment per unit cell of 14.6 μ_B along the crystallographic '*c*' axis and 2.56 μ_B along the tetragonally equivalent '*a*' and '*b*' axes.

A multipole deformation model for the analysis of spin density distributions in transition metal clusters has recently been described (Varghese & Mason 1980). It follows closely the methods established in the context of X-ray determination of molecular charge densities (Stewart 1973; 1976).

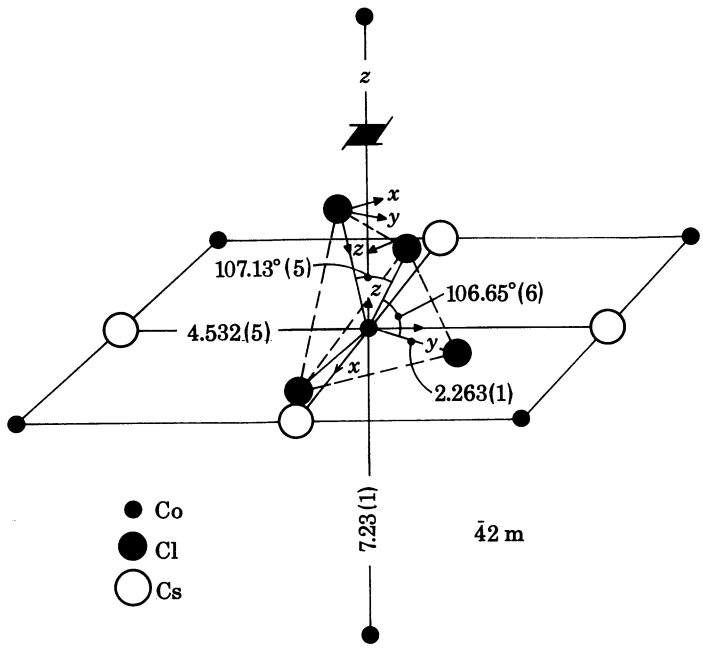

FIGURE 8. The local environment of the Co^{2+} ion in Cs_3CoCl_5. The distances (Å) and the angles are from the structure determination at 4.2 K. The local Cartesian axes used for the multipole analysis lie in the [110] mirror planes, and are related to each other by the point group symmetry at the Co^{2+} site ($\bar{4}2$m).

TABLE 2. TESSERAL HARMONICS (ANGULAR PART OF MULTIPOLE DENSITIES) AND NORMALIZATION CONSTANTS ASSOCIATED WITH THE NON-VANISHING MULTIPOLE POPULATIONS USED IN THE ANALYSIS OF Cs_3CoCl_5 IN TERMS OF THE DIRECTION COSINES (x, y, z) OF THE BRAGG VECTOR RELATIVE TO THE LOCAL CARTESIAN AXES OF THE CENTRES

(The notation used is that of Varghese & Mason (1980).)

l	m	M_l^m	$N_l^m/4\pi$
0	0	1	$1/4\pi$
1	−1	y	0.31831
1	0	z	0.31831
2	−1	$3yz$	0.25
2	0	$\frac{1}{2}(3z^2-1)$	0.4135
2	2	$(3x^2-y^2)$	0.125
3	−2	$30(xyz)$	0.06667
4	0	$\frac{5}{8}(7z^4-6z^2-\frac{3}{5})$	0.55534
4	4	$105(x^4-6y^2+y^4)$	0.004464

The local Cartesian systems centred on the cobalt and chlorine centres are indicated in figure 8; the y and z axes labelling the ligand atoms lie on crystallographic mirror planes. Relative to these Cartesian systems, the non-vanishing multipoles on the cobalt are the scalar M_0^0, the quadrupole M_2^0, the octupole M_3^{-2} and hexadecapoles M_4^0 and M_4^4; on the chlorine atoms we must account for the scalar M_0^0, the dipoles M_1^0 and M_1^{-1} and the quadrupoles M_2^0, M_2^{-1} and M_2^2. Table 2 lists the angular part of the corresponding multipole density function together with normalization factors; the notation is that of Varghese & Mason (1980).

TABLE 3. MULTIPOLE POPULATIONS (ELECTRONS) OF THE SPIN DENSITY DISTRIBUTION IN THE $[CoCl_4]^{2-}$ ION

(The statistical agreement factors are $R(F) = \Sigma|\Delta F|/\Sigma|F|$ and $\chi = \Sigma\omega\Delta F^2/(N-n)$, where $|\Delta F|$ is the difference between observed and calculated structure factors F, and the sum is over all N observed reflexions including the experimental bulk magnetization F_{000}. R_1 and R_2 refer to the refinements without and with a 4s density term on the cobalt centre, and $\delta\zeta/\zeta$ is the effective contraction or dilation factor of the scalar term M_0^0.)

		b-axis data		*c*-axis data	
centre	M_l^m l, m	R_1	R_2	R_1	R_2
Co	0, 0	2.39	2.38 (4)	2.53 (4)	2.50 (5)
	2, 0	0.04 (1)	0.04 (1)	−0.15 (3)	−0.27 (4)
	3, −2	0.12 (4)	0.11 (4)	0.13 (1)	0.12 (1)
	4, 0	−0.32 (3)	−0.30 (3)	−0.26 (5)	−0.17 (5)
	4, 4	−0.36 (5)	−0.40 (6)	−0.205 (7)	−0.219 (7)
	$\delta\zeta/\zeta$	0.144 (2)	0.153 (2)	0.160 (3)	0.200 (4)
	0, 0 (4s)		0.10 (6)		0.40 (4)
Cl	0, 0	0.18 (1)	0.17 (2)	0.066 (9)	0.35 (8)
	1, 0	−0.007 (5)	−0.006 (6)	0.007 (2)	−0.018 (2)
	1, −1	−0.003 (5)	−0.003 (5)	0.011 (3)	−0.001 (3)
	2, 0	−0.004 (6)	−0.005 (6)	0.002 (3)	−0.006 (3)
	2, −1	−0.02 (1)	−0.02 (1)	0.036 (8)	0.010 (9)
	2, 2	−0.004 (6)	−0.004 (6)	−0.002 (2)	0.006 (2)
	$\delta\zeta/\zeta$	−0.24 (2)	−0.25 (2)	−0.17 (2)	+0.25 (2)
	$R(F)$	0.051	0.051	0.037	0.029
	χ	1.269	1.260	2.370	2.049
	number of reflexions, N	111	111	78	78
	number of variables, n	13	14	13	14
	F_{000} cal./μ_B	2.561	2.561	12.98	14.15

TABLE 4. ORBITAL POPULATIONS (ELECTRONS) OF THE SPIN DENSITY DISTRIBUTION IN THE $[CoCl_4]^{2-}$ ION IN Cs_3CoCl_5, OBTAINED FROM THE MULTIPLE REFINEMENTS LISTED IN TABLE 3 BY USING THE TRANSFORMATION EQUATIONS OF VARGHESE & MASON (1980)

		b-axis data		*c*-axis data	
centre	orbital	R_1	R_2	R_1	R_2
Co	d_{z^2}	0.07 (6)	0.10 (5)	−0.02 (5)	−0.02 (5)
	$d_{x^2-y^2}$	−0.09 (8)	−0.26 (9)	0.28 (6)	0.40 (6)
	d_{xy}	0.93 (8)	0.99 (9)	0.92 (6)	1.08 (6)
	d_{xy}, d_{yz}	0.79 (3)	0.78 (3)	0.67 (6)	0.52 (6)
Cl	p_x	0.06 (1)	0.06 (1)	0.02 (1)	0.01 (1)
	p_y	0.06 (1)	0.05 (1)	0.03 (1)	0.01 (1)
	p_z	0.06 (1)	0.06 (1)	0.03 (1)	0.01 (1)

PHILOSOPHICAL TRANSACTIONS OF THE ROYAL SOCIETY B BIOLOGICAL SCIENCES

Radial wave functions are the self-consistent values for Co^{2+} (3d) and Cl (3p) given by Clementi & Roetti (1974). In the least squares analysis, the effective nuclear charge or the nephalauxetic effect ($\delta\zeta/\zeta$) was refined by taking a first-order Taylor expansion of the radial function. A scalar population $M_0^0(4s)$, with a self-consistent 4s radial function, was included in the final refinement.

Table 3 lists the results of the multipole population analysis while the interpretation of these populations, in terms of 'd' electron populations at the cobalt ion and '3p' electron density at the chlorines, is shown in table 4. If the spin density arises purely from one-centred d- and p-density functions on the metal and ligand centres respectively, then the multipoles M_3^{-2} (cobalt) and M_1^0, M_1^{-1} and M_2^{-2} (chlorine) should be negligible compared with others. The results are generally consistent with this expectation except that the dipole and quadrupole terms emerging from the '*c*' axis refinement are statistically significant and represent the projection of two-centre overlap density on to the ligand centres.

Both data sets confirm the t_2^3 configuration at the metal with an essentially spherically symmetric distribution of density at the ligands. Differing covalence implied from the '*b*' axis data refinement reflects, we believe, systematic errors in the analysis: there is a poorer sampling of ligand spin owing to the lower accuracy of scattering data relating to covalence (the '*c*' axis data contain (*hkl*) reflexions with *l* odd, which receive contributions only from the ligand atoms and any acentric density based on the cobalt ion).

There is a 15% contraction of the radial wave function of cobalt *vis-à-vis* the free ion value, the contraction results from both the transfer of spin to the ligands and the effect of the angular momentum contribution to the magnetization density. Within the dipole approximation (Marshall & Lovesey 1971), one expects a small modification to the radial part of the scalar density terms dependent on *g*: this has the effect of contracting the scalar density by approximately one-half that observed. It may be possible to infer that the orbital contribution to both data sets is similar on account of the similar *g* values and the magnitude of the orbital contractions in the two cases. This is a tentative conclusion that needs further study with more complete data and a clearer understanding of how our fitting approach may disguise an orbital contribution. Indeed, the apparently significant difference in population of the metal 3d(t) orbitals, which emerges from the '*c*' axis refinement, may be a direct indication of an inadequate modelling of orbital contributions.

Inclusion of a 4s density function in the analysis gives a markedly improved calculated bulk magnetization for the '*c*' axis data with a population of 0.40 (4) μ_B. This inclusion may sample the charge in the overlap region, a view which is supported by some *ab initio* calculations on the $(CoCl_4)^{2-}$ ion (Hillier *et al.* 1976). But we have not yet confirmed the uniqueness of an improved analysis with a 4s metal contribution compared with that resulting from including a δ-function on the metal.

The general conclusions are straightforward: the '*c*' axis data provide an accurate description of ligand and overlap densities while the '*b*' axis data give precise spin densities at the cobalt. The cobalt has the t_2^3 configuration, an orbital contraction of 8% and a net spin of 2.34 (4) μ_B; 0.07 (1) μ_B are transferred to the chlorine centre, the ligand density being essentially spherically symmetric. A plausible remaining interpretation is that the remaining spin (0.40 (4) μ_B is distributed in a diffuse metal 4s orbital.

PHILOSOPHICAL TRANSACTIONS OF THE ROYAL SOCIETY B BIOLOGICAL SCIENCES

References (Brown *et al.*)

Balcar, E., Lovesey, S. W. & Wedgewood, F. A. 1973 *J. Phys.* C **6**, 3746.
Bonnet, M., Delapalme, A., Becker, P. & Fuess, H. 1978 *J. Magn. magn. Mater.* **1**, 23.
Boucherle, J.-X. 1977 Thèse pour Docteur ès-sciences physiques, Université de Grenoble.
Brosset, C. 1938 *Z. anorg. allg. Chem.* **238**, 201.
Brown, P. J. & Forsyth, J. B. 1967 *Proc. phys. Soc.* **92**, 125.
Clementi, E. & Roetti, C. 1974 *Atom. data nucl. Data Tables* **14**, 177.
Cros, C., Dance, J.-M., Grenier, J.-C., Wanklyn, B. M. & Gerrard, B. J. 1977 *Mater. Res. Bull.* **12**, 415.
Figgis, B. N., Gerloch, M. & Mason, R. 1964 *Acta crystallogr.* **17**, 506.
Figgis, B. N., Mason, R., Reynolds, P. A., Smith, A. R. P., Varghese, J. N. & Williams, G. A. 1980*a* *J. chem. Soc. Dalton Trans.* (In the press.)
Figgis, B. N., Mason, R., Smith, A. R. P. & Williams, G. A. 1980*b* *Acta crystallogr.* (In the press.)
Figgis, B. N., Mason, R., Smith, A. R. P. & Williams, G. A. 1979 *J. Am. chem. Soc.* **101**, 3673.
Forsyth, J. B. & Brown, P. J. 1979 (In preparation.)
Hillier, I. H., Kendrick, J., Mabbs, F. E. & Garner, C. F. 1976 *J. Am. chem. Soc.* **98**, 395.
Hubbard, J. & Marshall, W. C. 1965 *Proc. phys. Soc.* **86**, 561.
Kostorz, G. & Mikhailovich, S. 1970 In *Proc. 12th Int. Conf. on Low Temp. Phys.*, p. 341. Academic Press of Japan.
Marshall, W. & Lovesey, S. W. 1971 In *Theory of thermal neutron scattering*, p. 156. Oxford University Press.
Moon, R. M. 1970 *Phys. Rev. Lett.* **25**, 527.
Moon, R. M., Koehler, W. C. & Cable, J. W. 1976 In *Proceedings of the Conference on Neutron Scattering*, Gatlinberg, Tennessee (CONF-760 601–P2) (ed. R. M. Moon), p. 577. National Technical Information Service, U.S. Department of Commerce, Springfield, Virginia.
Moon, R. M., Koehler, W. C. & Shull, C. G. 1975 *Nucl. Instrum. Meth.* **129**, 515.
Nathans, R., Shull, C. G., Shirane, G. & Andresen, A. 1959 *J. Phys. Chem. Solids* **10**, 138.
Radhakrishna, P. & Brown, P. J. 1980 *J. Phys.* F. **10**, 489.
Rakhecha, V. R. & Satya Murthy, S. N. 1978 *J. Phys.* C **11**, 4389.
van Stapele, R. P., Beljers, H. G., Bongers, P. F. & Zijlstra, H. 1966 *J. chem. Phys.* **44**, 3719.
Stassis, C. 1970 *Phys. Rev. Lett.* **24**, 1415.
Stewart, R. F. 1973 *J. chem. Phys.* **58**, 1668.
Stewart, R. F. 1976 *Acta crystallogr.* A **32**, 565.
Varghese, J. N. & Mason, R. 1980 *Proc. R. Soc. Lond.* A **372**, 1.
Wanklyn, B. M., Gerrard, B. J., Wondre, F. & Davidson, W. 1976 *J. Cryst. Growth* **33**, 165.

PHILOSOPHICAL TRANSACTIONS OF THE ROYAL SOCIETY B BIOLOGICAL SCIENCES